Electronic Supplementary Information for

A *pacs*-type metal-organic framework with high adsorption capacity for inverse C_2H_6/C_2H_4 separation

Kuo Zhang,[a] Jing-Jing Pang,[a] Xin Lian,[a] Zi-Han Song,[a] Yue-Chao Yuan,[a] Hongliang Huang,*[b] Zhao-Quan Yao,*[c] and Jian Xu*[a]

[a]*School of Materials Science and Engineering, Smart Sensing Interdisciplinary Science Center, TKL of Metal and Molecule-Based Material Chemistry, Nankai University, Tianjin 300350, China. Email: jxu@nankai.edu.cn*

[b]*School of Chemistry and Chemical Engineering, Tiangong University, Tianjin 300387, China. Email: huanghongliang@tiangong.edu.cn.*

[c]*School of Chemistry and Chemical Engineering, Tianjin University of Technology, Tianjin 300384, China. Email: yaozq@email.tjut.edu.cn.*

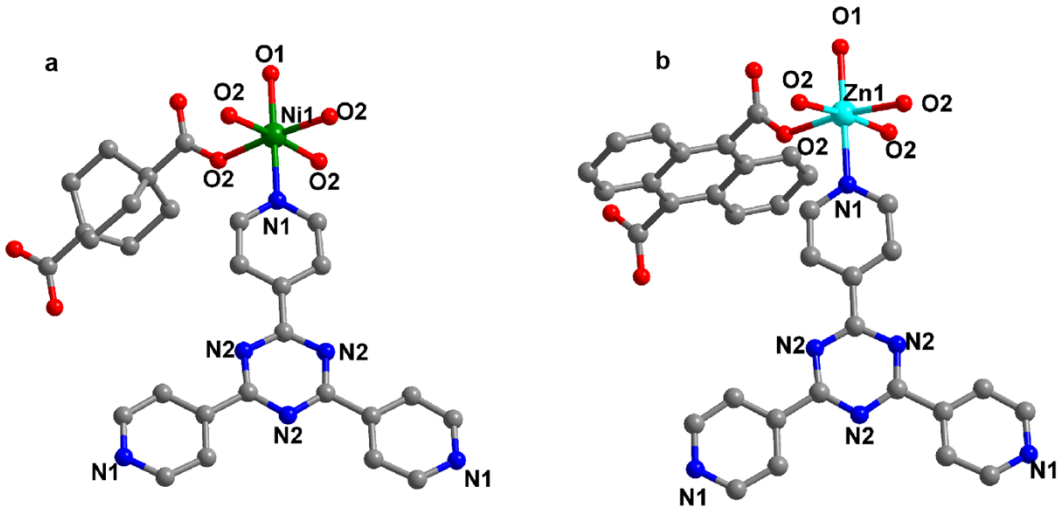

Fig. S1 (a) Coordination environment of Ni^{2+} ion in Ni-bodc-tpt. (b) Coordination environment of Zn^{2+} ion in Zn-adc-tpt. Hydrogen atoms are omitted, for clarity.

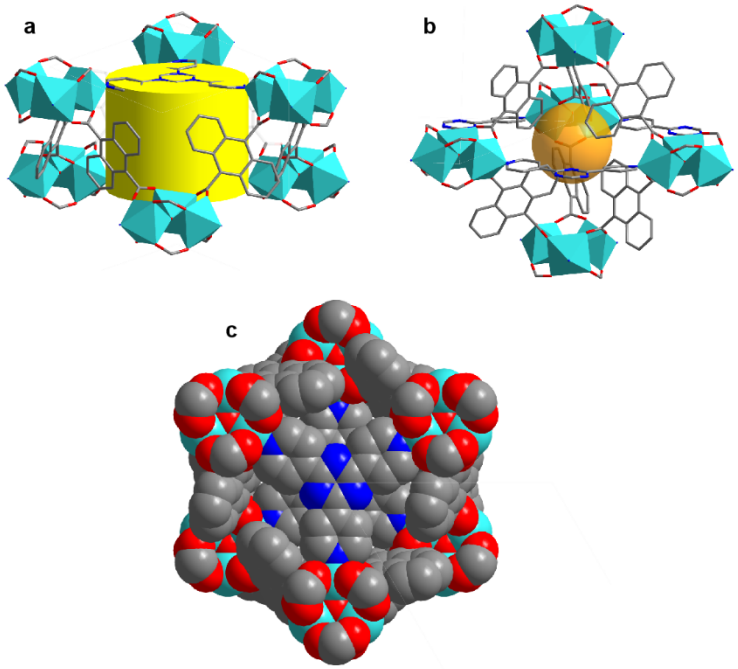

Fig. S2 (a and b) Cage A and B of Zn-adc-tpt. (c) View of the space-filling picture of Zn-adc-tpt along the *c* axis.

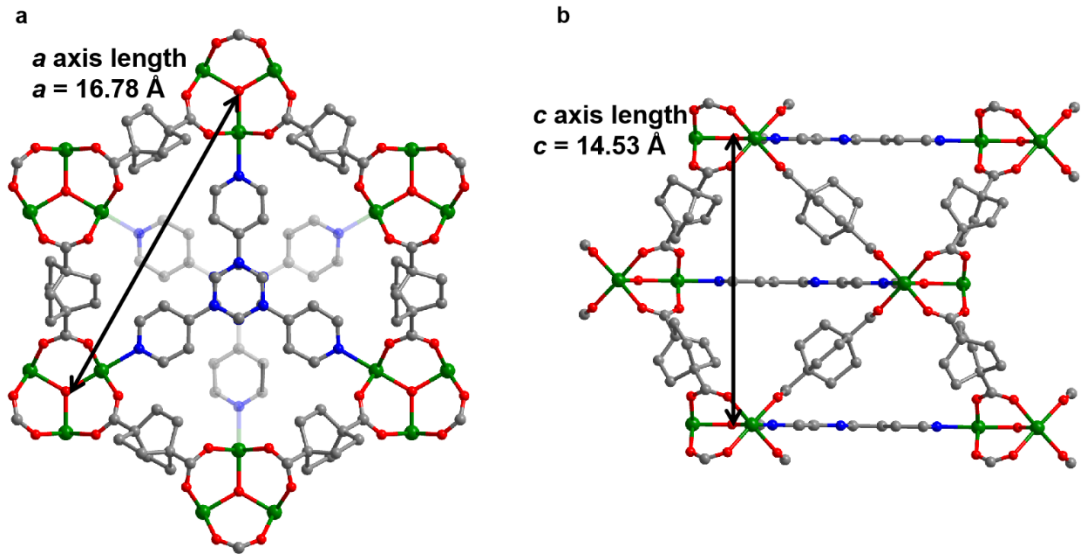

Fig. S3 (a) The horizontal distance between the μ_3-OH of the metal trimer SBU equal to the length of *a* axis. (b) The vertical distance between the μ_3-OH of the metal trimer SBU equal to the length of *c* axis.

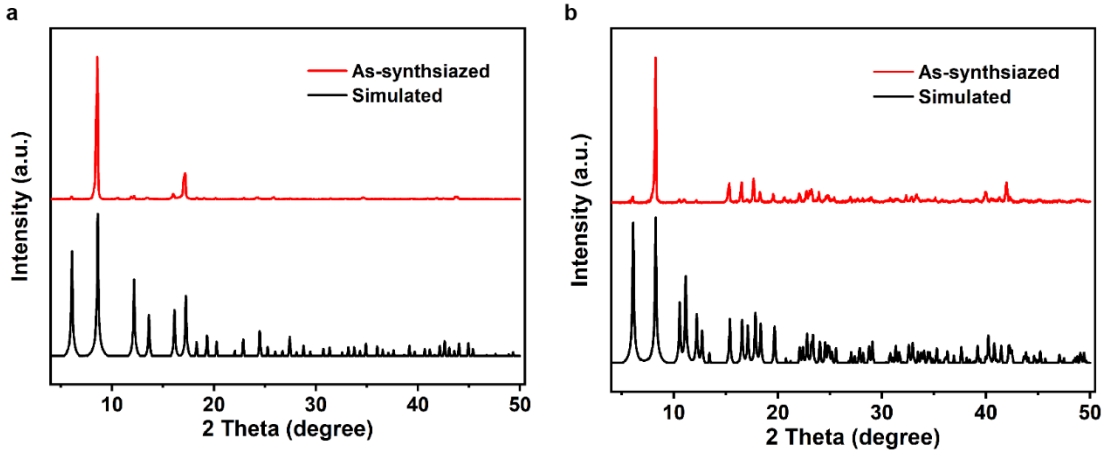

Fig. S4 PXRD data of Ni-bodc-tpt (a) and Zn-adc-tpt (b)

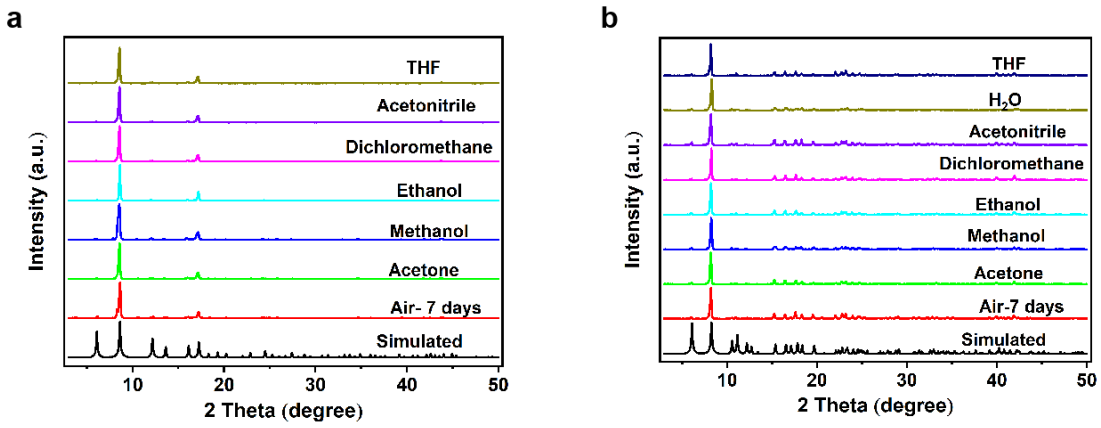

Fig. S5 PXRD patterns of Ni-bodc-tpt (a) and Zn-adc-tpt (b) after being soaked in different organic solvents for 24 h and exposure to air for 7 days.

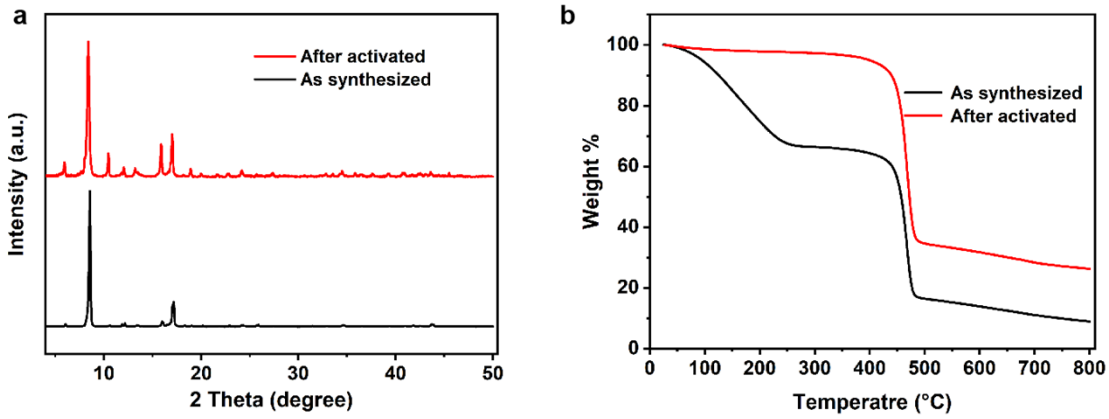

Fig. S6 PXRD data (a) and TGA curves (b) of the as-synthesized and activated samples of Ni-bodc-tpt.

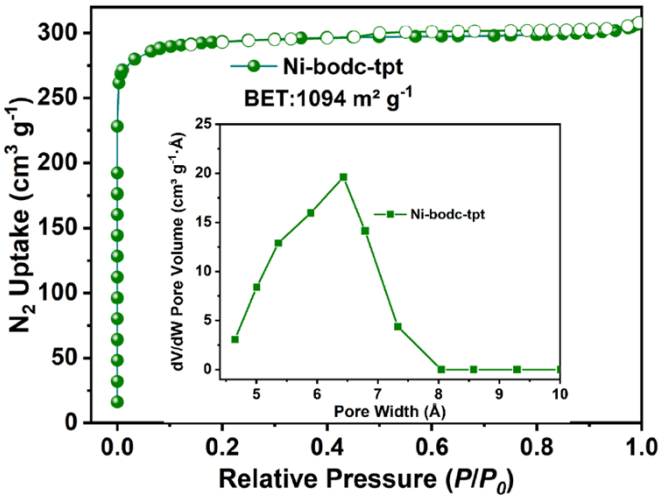

Fig. S7 N_2 adsorption-desorption isotherm on Ni-bodc-tpt at 77 K. Inset: the pore size distribution.

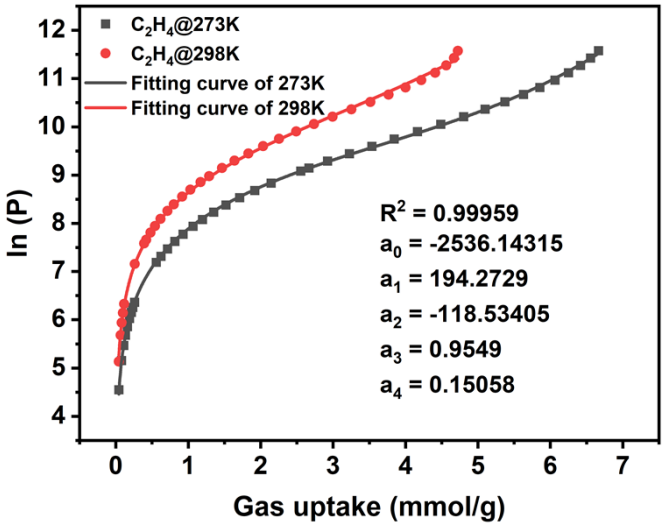

Fig. S8 Virial equation fitting of C_2H_4 adsorption isotherm of Ni-bodc-tpt at 273 and 298 K respectively.

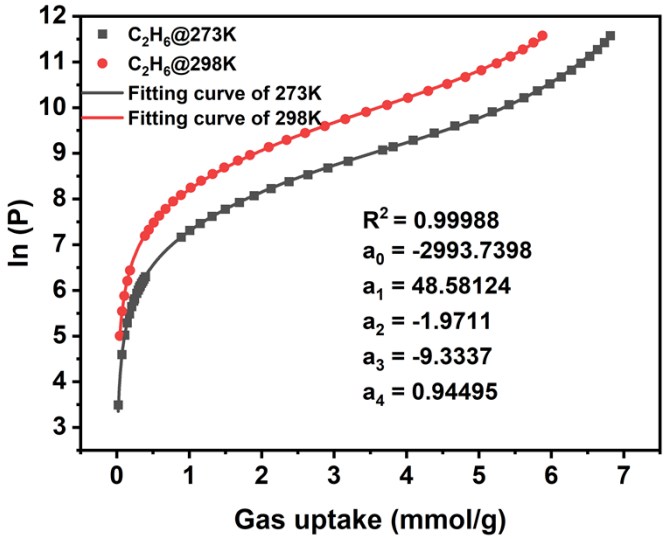

Fig. S9 Virial equation fitting of C_2H_6 adsorption isotherm of Ni-bodc-tpt at 273 and 298 K respectively.

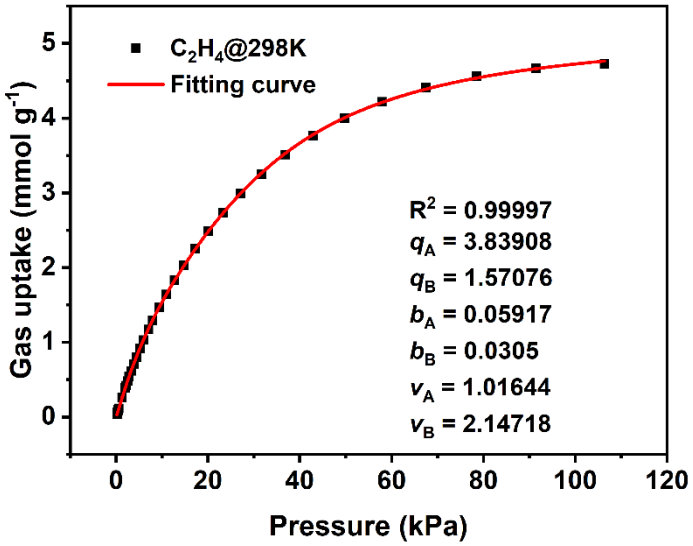

Fig. S10 Dual-site Langmuir-Freundlich fitting of C_2H_4 adsorption isotherm at 298 K for Ni-bodc-tpt.

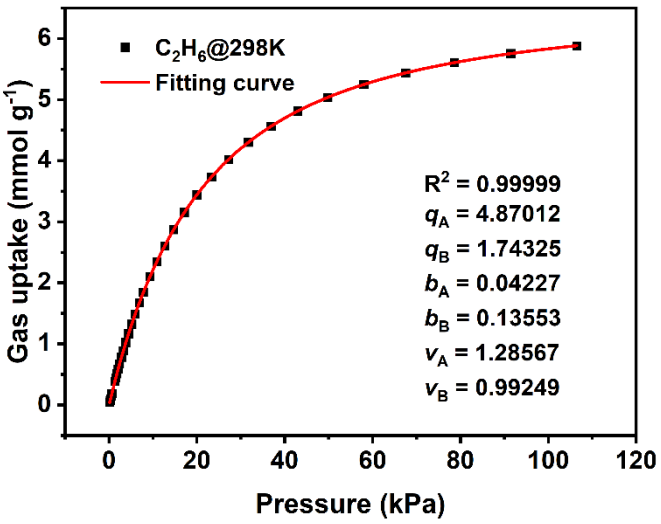

Fig. S11 Dual-site Langmuir-Freundlich fitting of C_2H_6 adsorption isotherm at 298 K for Ni-bodc-tpt.

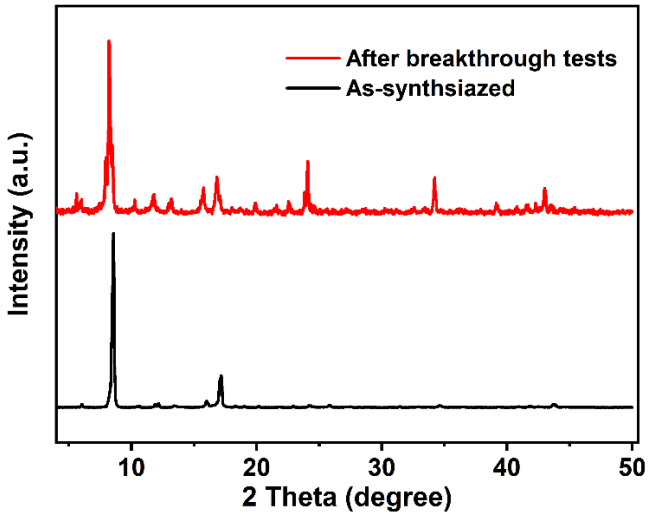

Fig. S12 PXRD of Ni-bodc-tpt after breakthrough tests.

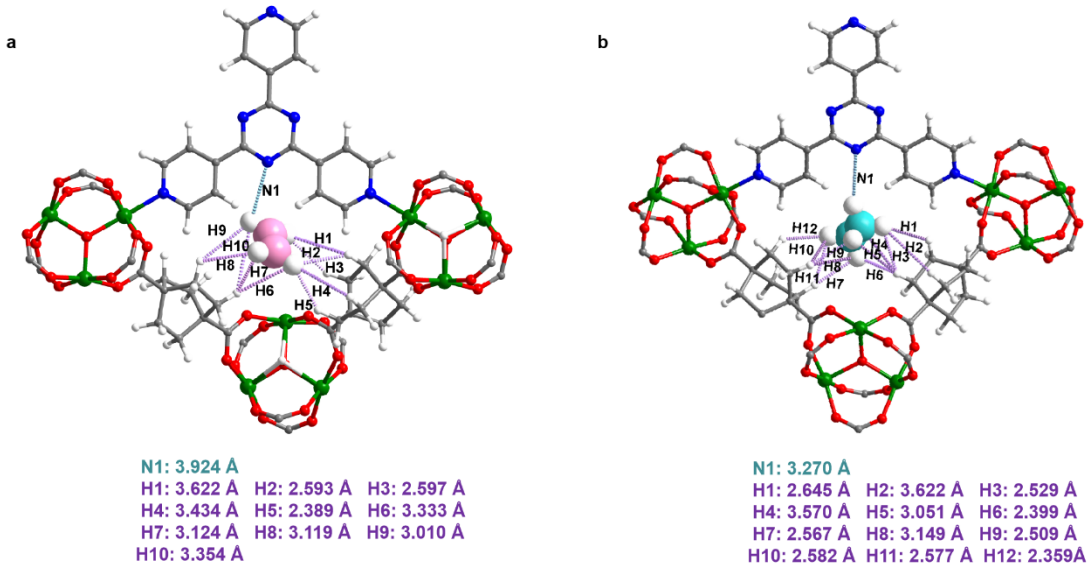

Fig. S13 Predicted adsorption sites and interactions of C_2H_4 (a) and C_2H_6 (b) in cage A of Ni-bodc-tpt. The blue dashed lines refer to C–H···N interactions while the purple ones refer to C–H···H interactions.

Table S1 Crystal data and structure refinement parameters for Ni-bodc-tpt.

Compound	Ni-bodc-tpt
CCDC number	2329063
Chemical formula	$C_{48}H_{48}N_6Ni_3O_{13}$
Crystal system	Hexagonal
Space group	$P6_3/mmc$
a/(Å)	16.7926(6)
b/(Å)	16.7926(6)
c/(Å)	14.6396(9)
α/(°)	90
β/(°)	90
γ/(°)	120
V/(Å^3)	3575.2(3)
Z	2
D/(g/cm^3)	1.015
T/K	210
F(000)	1132
Goodness-of-fit on F^2	1.173
R_1 [I >2σ(I)][a]	0.0689
R_1 [all data][a]	0.0780
wR_2 [I >2σ(I)][b]	0.2075
wR_2 [all data][b]	0.2255

[a]$R_1 = \sum||F_o| - |F_c|| / \sum|F_o|$; [b]$wR_2 = [\sum[w(F_o^2 - F_c^2)^2] / \sum w(F_o^2)^2]^{1/2}$.

Table S2 Crystal data and structure refinement parameters for Zn-adc-tpt.

Compound	Zn-adc-tpt
CCDC number	2329065
Chemical formula	$C_{66}H_{39}N_6Zn_3O_{13}$
Crystal system	Trigonal
Space group	*P*-31
a/(Å)	16.7370(2)
b/(Å)	16.7370(2)
c/(Å)	15.8689(3)
α/(°)	90
β/(°)	90
γ/(°)	120
V/(Å^3)	3849.75(12)
Z	2
D/(g/cm^3)	1.139
T/*K*	100
F(000)	1342
Goodness-of-fit on F^2	1.045
R_1 [I >2σ(I)][a]	0.0524
R_1 [all data][a]	0.0590
wR_2 [I >2σ(I)][b]	0.1373
wR_2 [all data][b]	0.1410

[a]$R_1 = \sum||F_o| - |F_c|| / \sum|F_o|$; [b]$wR_2 = [\sum[w(F_o^2 - F_c^2)^2] / \sum w(F_o^2)^2]^{1/2}$.

Table S3 Comparison of adsorption metrics of some benchmark C_2H_6-selective MOFs at 298 K and 1 bar.

MOF adsorbents	C_2H_6 uptake (mmol g^{-1})	C_2H_4 uptake (mmol g^{-1})	Selectivity (50/50, v/v)	Q_{st} of C_2H_6 (kJ mol^{-1})	Ref.
Ni-bodc-tpt	5.87	4.72	1.8	24.87	This work
$Fe_2(O_2)$(dobdc)	3.03	1.9	4.4	66.8	1
LIFM-63	2.89	2.07	1.56	26.5	2
$Ni(bdc)(ted)_{0.5}$	5.0	3.4	1.85	21.5	3
JNU-2	4.11	3.62	1.6	30	4
MUF-15	4.69	4.15	1.96	29.2	5
TKL-106	5.61	4.51	1.5	22.4	6
MIL-142A	3.8	2.9	1.5	27.2	7
$Cu(Qc)_2$	1.85	0.78	3.4	28.8	8
NUM-7	2.85	2.62	1.764	35.8	9
SNNU-40	7.54	4.91	1.57	18	10
CPM-233	7.45	6.52	1.64	27.3	11
PCN-250(Fe_2Co)	6.21	5.82	1.52	22.2	12

References

1. L. Li, R.-B. Lin, R. Krishna, H. Li, S. Xiang, H. Wu, J. Li, W. Zhou and B. Chen, *Science*, 2018, **362**, 443-446.
2. C. X. Chen, Z. W. Wei, T. Pham, P. C. Lan, L. Zhang, K. A. Forrest and S. Chen, *Angew. Chem. Int. Ed*., 2021, **60**, 9680–9685.
3. W. Liang, F. Xu, X. Zhou, J. Xiao, Q. Xia, Y. Li and Z. Li, *Chem. Eng. Sci*., 2016, **148**, 275–281.
4. H. Zeng, X. J. Xie, M. Xie, Y. L. Huang, D. Luo, T. Wang, Y. Zhao, W. Lu and D. Li, *J. Am. Chem. Soc*., 2019, **141**, 20390–20396.
5. O. T. Qazvini, R. Babarao, Z. L. Shi, Y. B. Zhang and S. G. Telfer, *J. Am. Chem. Soc*., 2019, **141**, 5014–5020.
6. M.-H. Yu, H. Fang, H.-L. Huang, M. Zhao, Z.-Y. Su, H.-X. Nie, Z. Chang and T.-L. Hu, *Small*, 2023, **19**, 2300821.
7. Y. Chen, H. Wu, D. Lv, R. Shi, Y. Chen, Q. Xia, Z. Li, *Ind. Eng. Chem. Res.,* 2018, **57**, 4063.
8. R.-B. Lin, H. Wu, L. Li, X.-L. Tang, Z. Li, J. Gao, H. Cui, W. Zhou, B. Chen, *J. Am. Chem. Soc.*, 2018, **140**, 12940.
9. F.-Z. Sun, S.-Q. Yang, R. Krishna, Y.-H. Zhang, Y.-P. Xia, T.-L. Hu, A*CS Appl. Mater. Interfaces,* 2020, **12**, 6105.
10. Y.-P. Li, Y.-N. Zhao, S.-N. Li, D.-Q. Yuan, Y.-C. Jiang, X. Bu, M.-C. Hu, Q.-G. Zhai, *Adv. Sci.*, 2021, **8**, 2003141.
11. H. Yang, Y. Wang, R. Krishna, X. Jia, Y. Wang, A. N. Hong, C. Dang, H. E. Castillo, X. Bu, P. Feng, *J. Am. Chem. Soc.,* 2020, **142**, 2222.
12. H. Wu, Y. Chen, Y. Yuan, D. Lv, S. Tu, Z. Liu, Z. Li, Q. Xia, *AIChE J.*, 2022, **68**, e17385